

State and Control Constrained Analytical Solution for Energy-Optimal Coordination of Connected and Automated Vehicles

A M Ishtiaque Mahbub, *Student Member, IEEE*, Andreas A. Malikopoulos, *Senior Member, IEEE*

Abstract—Connected and automated vehicles (CAVs) provide the most intriguing opportunity to reduce pollution, energy consumption, and travel delays. Previous works addressed the optimal coordination of CAVs using Hamiltonian analysis with relaxed state and control constraints. In this paper, we investigate the nature of the unconstrained problem and provide conditions under which the constraints become active. We derive closed form analytic solution of the state and control constrained optimization problem and evaluate the validity of the proposed solution using numerical simulation.

I. INTRODUCTION

The implementation of automated transportation system with connected automated vehicles (CAVs) enables novel computational framework to provide real-time control actions that optimizes energy consumption and associated advantages. From a control point of view, CAVs can alleviate congestion at major transportation segments [1], reduce emission, improve fuel efficiency [2], [3], and increase passenger safety. Partially constrained optimal control of CAV dynamics reduces computational complexity, but may lead to degraded performance metrics in real-world application. Particularly, vehicle speed and acceleration/deceleration constraints directly affect the physical limitations of the system, traffic regulations and passenger comfort. Therefore, we need to address the problem of optimal control of CAV dynamics with hard constraint on vehicle state and control.

Intersections, merging roadways, roundabouts, and speed reduction zones along with the driver responses to various disturbances [4] are the primary sources of bottlenecks that contribute to traffic congestion. Several research efforts have been reported in the literature proposing either centralized or decentralized approaches on coordinating CAVs through the conflict zone to improve traffic condition. One of the very early efforts in this direction was proposed in 1969 by Athans [5] for safe and efficient coordination of merging maneuvers with the intention to avoid congestion. In 2004, Dresner and Stone [6] proposed the use of the reservation scheme to control a single-free intersection of two roads. Since then, several research efforts have extended this approach [7]–[9]. Some approaches have focused on coordinating vehicles at intersections to improve the traffic flow [10]–[12]. Space constraints limit the inclusion and detailed description of the rich literature in this area, and thus, we limited our

efforts to reference work important for understanding the fundamental concepts or explaining significant departures from previous work. A recent survey paper [13] includes detailed discussions of the research reported in the literature to date on coordination of CAVs to improve vehicle-level operation.

More recently, an optimal control framework was established for coordinating online CAVs in different transportation segments. A closed-form, analytical solution without considering state and control constraints was presented in [14]–[16] for coordinating online CAVs at highway on-ramps, in [17] at intersections, and in [18] at roundabouts. The solution of the unconstrained problem was also validated experimentally using ten robotic CAVs [19] in a merging roadway scenario. The solution to the state and control unconstrained optimization problem discussed above shows acceleration spikes (jerk) at the boundaries of the solution, possibly exceeding the vehicle’s physical limitation and giving rise to undesired passenger discomfort. Additionally, the unconstrained optimal solution only abides by the roadway speed limit at the predefined terminal points and fails to maintain the roadway regulation within the control zone.

Therefore, the unconstrained optimal solution may be inadmissible in real-world application. To mitigate terminal jerk, Ntousakis, Nikolos, and Papageorgiou [16] reformulated the optimal control problem with vehicle acceleration as an additional state and jerk as the control input. The optimal control problem considering state and control constraints was addressed in [3] at an urban intersection without considering rear-end collision avoidance constraint. The conditions under which the latter does not become active were presented in [20]. We use the formulation presented in [3] further to provide useful insights about the state and control constraint activation and derive closed form analytic solution using the Hamiltonian analysis.

In this paper, we (1) provide conditions under which the state and control constraints do not become active and the conditions under which the specific constraints become active, and (2) derive a closed form analytical solution for the constrained optimization problem under different cases. Finally, we validate the analysis and the derived optimal solution using simulation.

The remainder of the paper is organized as follows. In Section II, we introduce the general optimization problem formulation and present the unconstrained case. In Section III, we discuss different aspects of the state and control constrained formulation in detail. In Section IV, we provide the analytic solution of the constrained optimization. In

This research was supported by ARPAC’s NEXTCAR program under the award number DE-AR0000796.

The authors are with the Department of Mechanical Engineering, University of Delaware, Newark, DE 19716 USA (emails: mahbub@udel.edu; andreas@udel.edu.)

Section V, we evaluate validity of the proposed approach in a simulation environment. We draw conclusions and discuss next steps in Section VI.

II. PROBLEM FORMULATION

We consider a network of CAVs driving through a roadway containing an arbitrary conflict zone, where possible collision may occur. Upstream of the conflict zone, we define a *control zone* where CAVs can coordinate with each other before they pass the conflict zone. The network has a coordinator that can communicate with the CAVs traveling inside the control zone. Note that the coordinator is not involved in any decision making process. Its purpose is to assign a unique identity to each CAV when they enter a control zone. When a vehicle enters the control zone, the coordinator receives its information and assigns a unique identity $i \in \mathbb{N}$ to the vehicle. We denote the queue of the vehicles to be entering the merging zone as $\mathcal{N}(t)$. The objective of each CAV is to derive its optimal control input (acceleration/deceleration) to cross the conflict zone avoiding collision with the other vehicles, and with hard constraint on its state and control.

A. Vehicle Dynamics and Constraints

Each vehicle $i \in \mathcal{N}(t)$ is modeled as a double integrator

$$\begin{aligned}\dot{p}_i &= v_i(t) \\ \dot{v}_i &= u_i(t)\end{aligned}\quad (1)$$

where $p_i(t) \in \mathcal{P}_i$, $v_i(t) \in \mathcal{V}_i$, and $u_i(t) \in \mathcal{U}_i$ denote the position, speed and acceleration/deceleration (control input) of each vehicle i in the corridor. The sets \mathcal{P}_i , \mathcal{V}_i , and \mathcal{U}_i , $i \in \mathcal{N}(t)$, are complete and totally bounded subsets of \mathbb{R} . Let $\mathbf{x}_i(t) = [p_i(t) \ v_i(t)]^T$ denote the state vector of each vehicle i , with initial value $\mathbf{x}_i^0 = [p_i^0 \ v_i^0]^T$ taking values in $\mathcal{X}_i = \mathcal{P}_i \times \mathcal{V}_i$. The state space \mathcal{X}_i for each vehicle i is closed with respect to the induced topology on $\mathcal{P}_i \times \mathcal{V}_i$ and thus, it is compact.

To ensure that the control input and vehicle speed are within a given admissible range, the following constraints are imposed.

$$\begin{aligned}u_{min} &\leq u_i(t) \leq u_{max}, \quad \text{and} \\ 0 &\leq v_{min} \leq v_i(t) \leq v_{max}, \quad \forall t \in [t_i^0, t_i^f],\end{aligned}\quad (2)$$

where u_{min} , u_{max} are the minimum deceleration and maximum acceleration for each vehicle $i \in \mathcal{N}(t)$, and v_{min} , v_{max} are the minimum and maximum speed limits respectively. t_i^0 is the initial time that vehicle i enters the first control zone in the corridor, and t_i^f is the time that vehicle i exits the corridor.

To ensure the absence of rear-end collision of two consecutive vehicles traveling on the same lane, the position of the preceding CAV k should be greater than or equal to the position of the following vehicle i plus a predefined safe distance $\delta_i(t)$. Thus we impose the rear-end safety constraint

$$s_i(t) = p_k(t) - p_i(t) \geq \delta_i(t), \quad \forall t \in [t_i^0, t_i^f], \quad (3)$$

where $s_i(t)$ denotes the distance of vehicle i from vehicle k which is physically immediately ahead of i , and $\delta_i(t)$ minimum safe distance which is a function of speed $v_i(t)$.

For each CAV $i \in \mathcal{N}(t)$, the lateral collision is possible within the set Γ_i ,

$$\Gamma_i \triangleq \{t \mid t \in [t_i^m, t_i^f]\}. \quad (4)$$

Lateral collision between any two CAVs $i, j \in \mathcal{N}(t)$ can be avoided if the following constraint hold,

$$\Gamma_i \cap \Gamma_j = \emptyset, \quad \forall t \in [t_i^m, t_i^f], \quad i, j \in \mathcal{N}(t). \quad (5)$$

In the modeling framework described above, we impose the following assumptions:

Assumption 1: For each CAV i , none of the constraints is active at t_i^0 .

Assumption 2: Each vehicle is equipped with sensors to measure and share their local information while communication among CAVs occurs without any delays or errors.

Assumption 3: The final endpoint constraint for the speed is not enforced for any CAV i .

Assumption 1 ensures that the initial state and control input are feasible. Assumption 2 may be strong, but it is relatively straightforward to relax as long as the noise in the measurements and/or delays is bounded. For example, we can determine upper bounds on the state uncertainties as a result of sensing or communication errors and delays, and incorporate these into more conservative safety constraints. As we do not consider any exit speed limit for the CAVs upon exiting the control zone, Assumption 3 enables us to focus only on the case where the final endpoint speed constraint is not enforced. Based on the enforcement of the endpoint speed constraint, we can have two different approaches towards solving the constrained optimization problem. Assumption 3 may be relaxed to include both cases in the future work.

B. Upper Level Vehicle Coordination

Let $N(t) \in \mathbb{N}$ be the number of CAVs inside the control zone at time $t \in \mathbb{R}^+$. When a vehicle enters the control zone, the coordinator receives its information and assigns a unique identity i to the vehicle. We denote the sequence of the vehicles to be entering the merging zone as $\mathcal{N}(t) = 1, \dots, N(t)$ and refer to this as the merging sequence. The sequence $\mathcal{N}(t)$ can be the outcome of an upper-level optimization problem. In what follows, we assume that the solution of the upper-level problem for determining the time t_i^m that each CAV enters the merging zone is given, and we will focus on a lower level control problem that will yield for each CAV the optimal control input (acceleration/deceleration) to achieve the assigned t_i^m .

C. Lower Level Energy Optimization Problem

For each vehicle $i \in \mathcal{N}(t)$ traveling inside the control zone, we formulate decentralized optimal control problem for each CAV i as,

$$\begin{aligned} \min_{u_i \in U_i} J_i(u(t)) &= \int_{t_i^0}^{t_i^m} C_i(u_i(t)) dt, \quad (6) \\ \text{subject to : (1), (2), } &p_i(t_i^0) = 0, p_i(t_i^m), \\ \text{and given } &t_i^0, v_i(t_i^0), t_i^m. \end{aligned}$$

Here, $C_i(u_i(t))$ is a function of the control input $u_i(t)$ and can be viewed as a measure of energy. When $C_i(u_i(t))$ is considered as the L^2 -norm of the control input, i.e. $C_i(u_i(t)) = \frac{1}{2}u_i^2(t)$, the transient engine operation can be minimized which, eventually, represents the minimization of energy consumption [3]. Note that, we do not provide any endpoint constraint of the speed $v_i(t_i^m)$ according to Assumption 3. Additionally, we do not explicitly include the safety constraints in (3) and (5). The lateral collision constraint (5) can be active only in the merging zone within $[t_i^m, t_i^f]$ according to (4). Therefore we enforce the lateral collision constraint by selecting the appropriate merging time t_i^m for each CAV i by solving the upper-level vehicle coordination problem. The rear-end collision constraint in (3), however, can be active any time $[t_i^0, t_i^m]$ within the control zone. The activation of (3) can be avoided under proper initial conditions $[t_i^0, v_i^0(t)]$ [3].

From (6) and the state equations (1), we construct the Hamiltonian function $H_i(t, \boldsymbol{\lambda}(t), \mathbf{x}(t), u(t))$ for each vehicle $i \in \mathcal{N}(t)$,

$$H_i(t, \boldsymbol{\lambda}(t), \mathbf{x}(t), u(t)) = \frac{1}{2}u_i^2 + \lambda_i^p \cdot v_i + \lambda_i^v \cdot u_i \quad (7)$$

where $\boldsymbol{\lambda}(t) = [\lambda_i^p \ \lambda_i^v]^T$ is the co-state vector consisting of the co-state components λ_i^p and λ_i^v corresponding to the state vector $\mathbf{x}_i(t)$. With the final terminal conditions at hand, we construct the endpoint Lagrangian $\bar{E}(t, \mathbf{x}(t), \boldsymbol{\nu})$,

$$\bar{E}(t, \mathbf{x}(t), \boldsymbol{\nu}) = \nu_i^1 (p_i^m - p_i(t_i^m)), \quad (8)$$

where, $\boldsymbol{\nu}$ is the endpoint co-vector containing a scalar multiplier ν_i^1 for including the only endpoint constraint given in (6). Including the safety constraints in (2), the Lagrangian of the Hamiltonian $L_i(t, \boldsymbol{\lambda}(t), \boldsymbol{\mu}(t), \mathbf{x}(t), u(t))$ with the state and control adjoined is,

$$\begin{aligned} L_i(t, \boldsymbol{\lambda}(t), \boldsymbol{\mu}(t), \mathbf{x}(t), u(t)) &= \frac{1}{2}u_i^2 \quad (9) \\ &+ \lambda_i^p \cdot v_i + \lambda_i^v \cdot u_i + \boldsymbol{\mu}^T \mathbf{g}(t, \mathbf{x}(t), u(t)) \\ &= \frac{1}{2}u_i^2 + \lambda_i^p \cdot v_i + \lambda_i^v \cdot u_i \\ &+ \mu_i^a \cdot (u_i - u_{max}) + \mu_i^b \cdot (u_{min} - u_i) \\ &+ \mu_i^c \cdot (v_i - v_{max}) + \mu_i^d \cdot (v_{min} - v_i), \quad \forall i \in \mathcal{N}(t) \end{aligned}$$

where, $\mathbf{g}(t, \mathbf{x}(t), u(t))$ holds the path constraints,

$$\mathbf{g}(t, \mathbf{x}(t), u(t)) = \begin{cases} u_i(t) - u_{max} \leq 0, \\ u_{min}(t) - u_i(t) \leq 0, \\ v_i(t) - v_{max} \leq 0, \\ v_{min}(t) - v_i(t) \leq 0, \end{cases} \quad (10)$$

and $\boldsymbol{\mu}^T$ is the path co-vector consisting of the Lagrange multipliers,

$$\mu_i^a = \begin{cases} > 0, & u_i(t) - u_{max} = 0, \\ = 0, & u_i(t) - u_{max} < 0, \end{cases} \quad (11)$$

$$\mu_i^b = \begin{cases} > 0, & u_{min} - u_i(t) = 0, \\ = 0, & u_{min} - u_i(t) < 0, \end{cases} \quad (12)$$

$$\mu_i^c = \begin{cases} > 0, & v_i(t) - v_{max} = 0, \\ = 0, & v_i(t) - v_{max} < 0, \end{cases} \quad (13)$$

$$\mu_i^d = \begin{cases} > 0, & v_{min} - v_i(t) = 0, \\ = 0, & v_{min} - v_i(t) < 0. \end{cases} \quad (14)$$

The Euler-Lagrange equations can be written as,

$$\dot{\lambda}_i^p(t) = -\frac{\partial L_i}{\partial p_i} = 0, \quad (15)$$

and

$$\dot{\lambda}_i^v = -\frac{\partial L_i}{\partial v_i} = \begin{cases} -\lambda_i^p, & v_i(t) - v_{max} < 0 \text{ and} \\ & v_{min} - v_i(t) < 0, \\ -\lambda_i^p + \mu_i^c, & v_i(t) - v_{max} = 0, \\ -\lambda_i^p - \mu_i^d, & v_{min} - v_i(t) = 0. \end{cases} \quad (16)$$

The necessary condition for optimality is

$$\frac{\partial L_i}{\partial u_i} = u_i + \lambda_i^v + \mu_i^a - \mu_i^b = 0. \quad (17)$$

D. Unconstrained Optimization

If the inequality state and control constraints (2) are not active, we have $\mu_i^a = \mu_i^b = \mu_i^c = \mu_i^d = 0$. Applying the necessary condition, the optimal control can be given

$$u_i(t) + \lambda_i^v = 0, \quad i \in \mathcal{N}(t). \quad (18)$$

From (15) and (16) we have $\lambda_i^p(t) = a_i$, and $\lambda_i^v(t) = -(a_i \cdot t + b_i)$. The coefficients a_i and b_i are constants of integration corresponding to each vehicle i . From (18) the optimal control input (acceleration/deceleration) as a function of time is given by

$$u_i^*(t) = a_i \cdot t + b_i, \quad \forall t \geq t_i^0. \quad (19)$$

Substituting the last equation into (1) we find the optimal speed and position for each vehicle, namely

$$v_i^*(t) = \frac{1}{2}a_i \cdot t^2 + b_i \cdot t + c_i, \quad \forall t \geq t_i^0 \quad (20)$$

$$p_i^*(t) = \frac{1}{6}a_i \cdot t^3 + \frac{1}{2}b_i \cdot t^2 + c_i \cdot t + d_i, \quad \forall t \geq t_i^0. \quad (21)$$

Here, a_i , b_i , c_i , and d_i are constants of integration. These four constants above can be computed by using the boundary conditions in (6). The analytic solution of the unconstrained optimization is illustrated Fig. 1.

III. CONSTRAINED OPTIMIZATION

To address the state and control constrained formulation of (9), we 1) identify the conditions for constraint(s) exclusion, 2) define the condition under which they become active, and 3) derive the constrained optimal solution, if one exists. In what follows, we introduce the necessary Lemmas, Theorems and associated proofs to follow the above steps.

A. Condition of Constraint Exclusion

Although we have two state constraints and two control constraints from (10), total 15 constraint combinations can be violated. We show in lemma 2 that under assumption 3, it is only possible for a subset of the constraints to be active within an unconstrained solution. Therefore, it is not necessary to consider all the cases while solving for the constrained problem. In what follows, we delve deeper into the nature of the unconstrained optimal arc to derive useful information about the possible existence of constraint violation within the control zone.

Lemma 1: If $v_i(t_i^m)$ is not fixed, then,

$$t_i^m = -\frac{b_i}{a_i}. \quad (22)$$

Proof: According to Assumption 3, we construct the endpoint Lagrangian $\bar{E}(t, \mathbf{x}(t), \boldsymbol{\nu})$ as in (8). We have the following terminal transversality conditions [21],

$$\lambda_i^p(t_i^m) = \frac{\partial \bar{E}}{\partial p_i} = \nu_i, \quad (23)$$

$$\lambda_i^v(t_i^m) = \frac{\partial \bar{E}}{\partial v_i} = 0. \quad (24)$$

Equation (23) provides no additional information which essentially equates two unknown covector elements. However, (24) provides a non-trivial boundary condition. Using the result of (24) in (19), we can write,

$$u_i(t_i^m) = a_i t_i^m + b_i = 0, \quad (25)$$

which gives, (22). Furthermore, as $t_i^m > t_0 \geq 0$, b_i and a_i always have different signs. ■

Lemma 2: The optimal acceleration profile is linearly decreasing if,

$$v_i^0 < \frac{(p_i(t_i^m) - p_i(t_i^0))}{t_i^m}. \quad (26)$$

Similarly, the optimal acceleration profile is linearly increasing if,

$$v_i^0 > \frac{(p_i(t_i^m) - p_i(t_i^0))}{t_i^m}. \quad (27)$$

Proof: From (20) and (21), we can write

$$v_i(t_i^0) = v_i^0 = \frac{1}{2}a_i(t_i^0)^2 + b_i t_i^0 + c_i. \quad (28)$$

$$p_i(t_i^0) = \frac{1}{6}a_i \cdot (t_i^0)^3 + \frac{1}{2}b_i \cdot (t_i^0)^2 + c_i \cdot t_i^0 + d_i. \quad (29)$$

With $t_i^0 = 0$, we get

$$c_i = v_i^0, \quad (30)$$

$$d_i = p_i(t_i^0). \quad (31)$$

Again from (21), we can write,

$$p_i(t_i^m) = \frac{1}{6}a_i(t_i^m)^3 + \frac{1}{2}b_i(t_i^m)^2 + c_i t_i^m + d_i. \quad (32)$$

Using the results from (30), (31) and (22) in (32) and solving for a_i , we get

$$a_i = \frac{3(v_0 t_i^m - (p_i(t_i^m) - p_i(t_i^0)))}{(t_i^m)^3}. \quad (33)$$

As $t_i^m > 0$, a_i is non positive if

$$v_i^0 t_i^m - (p_i(t_i^m) - p_i(t_i^0)) < 0, \quad (34)$$

which in turn implies negative slope of the acceleration profile, i.e., linearly decreasing acceleration profile. The second part of Lemma 2 can be proved following similar steps. ■

Lemma 3: For a given unconstrained optimal profile, only a subset of state-control constraints can remain active. Furthermore, if any element of the constraint pair $(v_i(t) - v_{max} \leq 0, u_i(t) - u_{max} \leq 0)$ is violated, none from the constraint pair $(v_{min} - v_i(t) \leq 0, u_i(t) - u_{min} \geq 0)$ can be violated. The reverse also holds.

Proof: The optimal solution derived from the unconstrained Hamiltonian analysis yields a linear control profile increasing or decreasing to the terminal value zero (Lemma 2). In the case where the acceleration profile is linearly decreasing, we have $u_i(t) = a_i t + b_i \geq 0 > u_{min}, \forall t \in [t_i^0, t_i^m]$, implying that the constraint $u_i(t) - u_{min}(t) \geq 0$ will never be violated. Thus, $\mu_i^b = 0, \forall t > t_i^0$ in (12). The corresponding quadratic velocity profile (20) is a parabolic function of degree 2 with Y-symmetric axis located at t_i^m in the speed-time profile. Applying the necessary and sufficient condition of optimality to (20), we get,

$$\frac{\partial v_i(t)}{\partial t} = a_i t + b_i = 0, \quad (35)$$

$$\frac{\partial^2 v_i(t)}{\partial t^2} = a_i. \quad (36)$$

Solving (35), we get the inflection point at $t = -\frac{b_i}{a_i}$ which corresponds to the vertex of the parabola of (20). Whether this point corresponds to the maximum or minimum of the (20) can be determined from the sufficient condition of (36). For $a_i < 0$, we have a maximum at the vertex, giving rise to a concave quadratic profile. As the inflection point is located at t_i^m and $v_{min} < v_i^0 < v_{max}$, we have $v_i(t) > v_{min}, \forall t \geq t_i^0$. Therefore, for a CAV with linearly decreasing unconstrained optimal acceleration profile, the constraint $v_i(t) - v_{min}(t) \geq 0$ and $u_i(t) - u_{min} \geq 0$ will never be violated. Similar approach can be taken to prove the second part of Lemma 3. ■

Remark 1: The sign of the constant a_i provides insight for the possible state and control constraint violation.

Based on Lemma 2 and 3, we now provide a Theorem which provides the condition under which the state and control constraints will not become active.

Theorem 1: The state constraint $v_i(t) - v_{min} \geq 0$ and the control constraint $u_i(t) - u_{min} \geq 0$ will not be violated when $v_i^0 < \frac{(p_i(t_i^m) - p_i(t_i^0))}{t_i^m}$ holds. Similarly, the state constraint $v_{max} - v_i(t) \geq 0$ and the control constraint $u_{max} - u_i(t) \geq 0$ will not be violated when $v_i^0 > \frac{(p_i(t_i^m) - p_i(t_i^0))}{t_i^m}$ holds.

Proof: If the condition $v_i^0 < \frac{(p_i(t_i^m) - p_i(t_i^0))}{t_i^m}$ holds, then according to Lemma 2, a_i is negative and the optimal acceleration profile is linearly decreasing. From Lemma 3, a decreasing acceleration profile indicates that the state constraint $v_i(t) - v_{min}(t) \geq 0$ and the control constraint

$u_i(t) - u_{min}(t) \geq 0$ will never be violated, which concludes the proof of the first part. The proof of the second part of Theorem 1 follows similar procedure. ■

B. Conditions of Constraint Violation

The following theorems provide the condition for which the violation of the state and control constraints exists.

Lemma 4: Violation of the control constraint $u_i(t) - u_{max} \leq 0$ or $u_i(t) - u_{min} \geq 0$ occurs at time $t = t_i^0$.

Proof: For $a_i < 0$, there is possibility of either the state constraint $v_i(t) - v_{max}(t) \leq 0$ or the control constraint $u_i(t) - u_{max} \leq 0$ or both to be violated (Lemma 3). In this case, Lemma 2 implies that the slope of the acceleration profile will be negative, i.e., linearly decreasing to zero. Therefore, any violation of the control constraint $u_i(t) - u_{max}(t) \leq 0$, if exists, will occur at time $t = t_i^0$. Similarly, it can be proved that the violation of $u_i(t) - u_{min} \geq 0$ occurs at time $t = t_i^0$. ■

Theorem 2: For $a_i < 0$, the state constraint $v_i(t) - v_{max}(t) \leq 0$ is violated if,

$$t_i^m < \frac{3(p_i(t_i^m) - p_i(t_i^0))}{v_i^0 + 2v_{max}}. \quad (37)$$

Similarly, for $a_i > 0$, the violation of the state constraint $v_i(t) - v_{min}(t) \geq 0$ exists if,

$$t_i^m > \frac{3(p_i(t_i^m) - p_i(t_i^0))}{v_i^0 + 2v_{min}}. \quad (38)$$

Proof: Let us consider that for $a_i < 0$, there exists a time $\tau_s \in [t_i^0, t_i^m]$ at which the state constraint $v_i(t) - v_{max}(t) \leq 0$ is violated. Using (30) as in Lemma 1, we write (20) as,

$$\frac{1}{2}a_i\tau_s^2 + b_i\tau_s + v_i^0 = v_{max}. \quad (39)$$

Solving for τ_s , we get

$$\tau_s = \frac{-2b_i \pm \sqrt{4b_i^2 - 8a_i(v_i^0 - v_{max})}}{2a_i}. \quad (40)$$

Using (22), we get two possible solutions of τ ,

$$\tau_s = t_i^m + \sqrt{\frac{4b_i^2 - 8a_i(v_i^0 - v_{max})}{4a_i^2}}, \quad (41)$$

$$\tau_s = t_i^m - \sqrt{\frac{4b_i^2 - 8a_i(v_i^0 - v_{max})}{4a_i^2}}. \quad (42)$$

Now, (41) cannot be admitted as $\sqrt{4b_i^2 - 8a_i(v_i^0 - v_{max})}$ cannot be negative or equal to zero to satisfy $\tau_s < t_i^m$. Therefore, (42) is the acceptable solution. Again, to satisfy $\tau_s < t_i^m$, $\sqrt{4b_i^2 - 8a_i(v_i^0 - v_{max})} > 0$. Simplifying, we get

$$a_i < \frac{2(v_i^0 - v_{max})}{t_i^2}. \quad (43)$$

Substituting (33) and simplifying, we get (37). By considering $a_i > 0$, the same procedure can be used to prove (38) of Theorem 2. ■

Theorem 3: For $a_i < 0$, control constraint $u_i(t) - u_{max}(t) \leq 0$ is violated if,

$$t_i^m < \frac{-3v_i^0 + \sqrt{9(v_i^0)^2 + 12u_{max}(p_i(t_i^m) - p_i(t_i^0))}}{2u_{max}}. \quad (44)$$

For $a_i > 0$, control constraint $u_{min} - u_i(t) \leq 0$ is violated if,

$$t_i^m > \frac{-3v_i^0 + \sqrt{9(v_i^0)^2 + 12u_{min}(p_i(t_i^m) - p_i(t_i^0))}}{2u_{min}}. \quad (45)$$

Proof: According to Lemma 4, the control constraint violation occurs at $t = t_i^0$. For $a_i < 0$, we have,

$$u_i(t_i^0) = a_i t_i^0 + b_i > u_{max}. \quad (46)$$

With $t_i^0 = 0$, we get $b_i = -a_i t_i^m > u_{max}$. Substituting the value of a_i (33) and simplifying, we obtain

$$u_{max}(t_i^m)^2 + 3v_i^0 t_i^m - 3(p_i(t_i^m) - p_i(t_i^0)) < 0. \quad (47)$$

Solving the quadratic term for t_i^m , we eventually get

$$\left(t_i^m + \frac{3v_i^0 + \sqrt{9(v_i^0)^2 + 12u_{max}(p_i(t_i^m) - p_i(t_i^0))}}{2u_{max}}\right) \left(t_i^m + \frac{3v_i^0 - \sqrt{9(v_i^0)^2 + 12u_{max}(p_i(t_i^m) - p_i(t_i^0))}}{2u_{max}}\right) < 0. \quad (48)$$

The first term of (48) is always positive as $\sqrt{9(v_i^0)^2 + 12u_{max}(p_i(t_i^m) - p_i(t_i^0))} > 0$. Therefore, the second part has to be negative which yields the condition stated in (44). For $a_i > 0$, (45) can be proved with similar procedure. ■

So far we have discussed the conditions under which the state and control constraints are violated individually. With this information at hand, we can solve the constrained optimization problem and derive corresponding analytical solution, which we will present in the following section. However, there is a possibility that the optimal solution might result in additional constraint violation that was nonexistent in the initial estimation. For example, the solution of the optimization problem with only state constraint might cause additional control constraint violation. Similarly, resolving the control constrained problem might result in state constraint violation. In such cases, the optimization problem has to be resolved with updated constraints to derive the corresponding analytic solution. As our goal is to derive and implement the solution online, this procedure is not computationally feasible. Therefore, we need to check beforehand under which condition these additional constraints may be violated.

Theorem 4: If the state constraint $v_i(t) - v_{max} \leq 0$ is violated at first, then the state constrained optimal solution results in additional control constraint $u_i(t) - u_{max} \leq 0$ violation if,

$$\tau_s < \frac{-3v_i^0 + \sqrt{9(v_i^0)^2 + 12u_{max}(p_i(\tau_s) - p_i(t_i^0))}}{2u_{max}}. \quad (49)$$

Here, τ_s is the time at which the state constraint transitions from unconstrained to the constrained arc and can be calculated from the terminal conditions. Similarly, if the state

constraint $v_i(t) - v_{min} \geq 0$ is violated at first, then the state constrained optimal solution results in an additional control constraint $u_i(t) - u_{min} \geq 0$ violation if,

$$\tau_s > \frac{-3v_i^0 + \sqrt{9(v_i^0)^2 + 12u_{min}(p_i(\tau_s) - p_i(t_i^0))}}{2u_{min}}. \quad (50)$$

Proof: Let's assume that the state constraint $v_i(t) - v_{max} \geq 0$ is violated at $t = \tau_s$. The state constrained optimal solution yields a linear acceleration profile that has to enter the constrained arc at $t = \tau_s$ with $u_i(\tau_s) = 0$. As a result, we can focus on the unconstrained state and control trajectory with reduced time horizon $t \in [t_i^0, \tau_s]$ instead of $[t_i^0, t_i^m]$. Following the same procedure from the proof of theorem 4, we can construct the condition (49) that indicates whether the control constraint $u_i(t) - u_{max} \leq 0$ is being violated within the modified horizon $t \in [t_i^0, \tau_s]$. The second part of Theorem 4 can be proved following similar procedure. ■

Theorem 6: If the control constraint $u_i(t) - u_{max} \leq 0$ is violated first, then the control constrained optimal solution results in additional state constraint $v_i(t) - v_{max} \leq 0$ violation if the following holds,

$$t_i^m < \tau_c + \frac{3(p_i(t_i^m) - p_i(\tau_c))}{v_i^0 + u_{max}\tau_c + 2v_{max}}. \quad (51)$$

Here, τ_c is the time at which the control constraint transitions from the constrained to the unconstrained arc. Similarly, If the control constraint $u_i(t) - u_{min} \geq 0$ is violated first, then the control constrained optimal solution results in additional state constraint $v_i(t) - v_{min} \geq 0$ violation if the following holds,

$$t_i^m > \tau_c + \frac{3(p_i(t_i^m) - p_i(\tau_c))}{v_i^0 + u_{min}\tau_c + 2v_{min}}. \quad (52)$$

Proof: Let's assume that the control constraint $u_i(t) - u_{max} \leq 0$ is violated at first. The control constrained optimal solution yields an acceleration profile that has leaves the constrained arc at $t = \tau_c > t_i^0$ with $u_i(\tau_c) = u_{max}$. Therefore, we can focus on the unconstrained state and control trajectory with reduced time horizon $t \in [\tau_c, t_i^m]$ instead of $[t_i^0, t_i^m]$. Following the same procedure as in the proof of theorem 2, we can construct the condition (49). Similarly, (52) can be proved. ■

IV. ANALYTICAL SOLUTION OF CONSTRAINED OPTIMIZATION

To derive the analytical solution of (6) using Hamiltonian analysis, we follow the standard methodology used in optimal control problems with control and state constraints [22] and [21]. We first start with Theorem 1 to reduce the set of possible constraint violations. Then we evaluate the conditions in Theorem 2 and 3 to check for possible constraint violation. If no violation is identified, we simply derive the unconstrained arc. Otherwise, we solve the problem with the unconstrained arc and the arc corresponding to the violated constraint pieced together. The two arcs yield a set of algebraic equations which are solved simultaneously using the boundary conditions of and interior conditions between the arcs. We then use Theorem 4 or 5 to identify any additional constraint violation that might ensue from the

previous solution. If additional constraint violation exists, the last two arcs are pieced together with the arc corresponding to the new violated constraint, and we re-solve the problem with the three arcs pieced together.

We now consider the different cases of state and control constraint violations to derive the optimal profile for the CAVs. Due to space limitation, we only present derivation pertaining to the state constraint $v_i(t) - v_{max}(t) \leq 0$ and control constraint $u_i(t) - u_{max}(t) \leq 0$ violation.

Case 1: If only the state constraint $v_i(t) - v_{max} \leq 0$ is violated, we have $\mu_i^a = \mu_i^b = \mu_i^d = 0$. The corresponding necessary condition for optimality, and the Euler-Lagrangian equations (15) and (16) for the costates become

$$u_i + \lambda_i^v = 0, \quad (53)$$

$$\dot{\lambda}_i^p = 0, \quad (54)$$

$$\dot{\lambda}_i^v = -\lambda_i^p + \mu_i^c. \quad (55)$$

Let us assume that at a time τ_s such that $t_i^0 < \tau_s < t_i^m$, the state constraint is violated. We have an interior boundary condition $\mathbf{h}(t, \mathbf{x}(t), u(t)) = v_i(\tau_s) - v_{max} = 0$, and have a three-point boundary value problem. Therefore, at $t = \tau_s$, the state enters the constrained arc with $v_i(t) = v_{max}$. We denote τ_s^- and τ_s^+ as the immediate left and the right side of τ_s . At this entry point, we need to consider the jump conditions to asses the discontinuities of the costates and Hamiltonian as,

$$\boldsymbol{\lambda}(\tau_s^-) - \boldsymbol{\lambda}(\tau_s^+) = \boldsymbol{\eta}^T \frac{\partial \mathbf{g}}{\partial \mathbf{x}} \Big|_{t=\tau_s}, \quad (56)$$

$$H(\tau_s^+) - H(\tau_s^-) = \boldsymbol{\eta}^T \frac{\partial \mathbf{g}}{\partial t} \Big|_{t=\tau_s}, \quad (57)$$

$$(58)$$

where, $\boldsymbol{\eta}^T$ is a vector of Lagrange multipliers. Using (56) and (57), we determine the jump conditions of the costates and the Hamiltonian,

$$\lambda_i^p(\tau_s^-) - \lambda_i^p(\tau_s^+) = \eta_1 \frac{\partial(v_i(\tau_s) - v_{max})}{\partial p_i(t)} = 0, \quad (59)$$

$$\lambda_i^v(\tau_s^-) - \lambda_i^v(\tau_s^+) = \eta_2 \frac{\partial(v_i(\tau_s) - v_{max})}{\partial v_i(t)} = \eta_2, \quad (60)$$

$$H(\tau_s^+) - H(\tau_s^-) + \eta_3 \frac{\partial(v_i(\tau_s) - v_{max})}{\partial t} = 0, \quad (61)$$

According to (59) and (61), both the position costate and the Hamiltonian is continuous at $t = \tau_s$. If $u_i(\tau_s^+) = 0$, then (61) yields $u_i(\tau_s^-) = 0$, which implies that $\lambda_i^v(t)$ is also continuous at $t = \tau_s$ and $\eta_2 = 0$ in (60). Therefore, from (55), we have

$$\mu_i^c(t) = \begin{cases} = 0, & \text{if } v_i(t) < v_{max}, \\ = -\lambda_i^p, & \text{if } v_i(t) = v_{max}. \end{cases} \quad (62)$$

Using (53),(54), (55), (62), the initial, final conditions, and the terminal transversality condition at $t = t_i^m$, we now formulate a closed form analytic solution stitching the

unconstrained and constrained arcs together at $t = \tau_s$.

$$\begin{pmatrix} \frac{(t_i^0)^2}{2} & (t_i^0) & 1 & 0 & 0 & 0 & 0 & 0 \\ \frac{(t_i^0)^3}{6} & \frac{(t_i^0)^2}{2} & t_i^0 & 1 & 0 & 0 & 0 & 0 \\ \tau & 1 & 0 & 0 & -\tau_s & -1 & 0 & 0 \\ \frac{\tau^2}{2} & \tau_s & 1 & 0 & 0 & 0 & 0 & 0 \\ \tau & 1 & 0 & 0 & 0 & 0 & 0 & 0 \\ \frac{\tau^2}{2} & \tau_s & 0 & 0 & -\frac{\tau_s^2}{2} & -\tau_s & 0 & 0 \\ 0 & 0 & 0 & 0 & \frac{(t_i^m)^3}{6} & \frac{(t_i^m)^2}{2} & t_i^m & 1 \\ 0 & 0 & 0 & 0 & t_i^m & 1 & 0 & 0 \end{pmatrix} \cdot \begin{pmatrix} a_i \\ b_i \\ c_i \\ d_i \\ e_i \\ f_i \\ g_i \\ h_i \end{pmatrix} = \begin{pmatrix} p_i(t_i^0) \\ v_i(t_i^0) \\ 0 \\ v_{max} \\ 0 \\ 0 \\ p_i(t_i^m) \\ 0 \end{pmatrix}, \forall t \geq t_i^0, \quad (63)$$

where a_i, b_i, c_i, d_i are the constants of integration for the unconstrained arc, and g_i, h_i, q_i, w_i are the constants of integration for the constrained arc.

Case 2: If only the control constraint $u_i(t) - u_{max} \leq 0$ is violated, we have $\mu_i^b = \mu_i^c = \mu_i^d = 0$. The corresponding necessary condition for optimality, and the Euler-Lagrangian equations (15) and (16) for the costates become

$$u_i + \lambda_i^v + \mu_i^a = 0, \quad (64)$$

$$\dot{\lambda}_i^p = 0, \quad (65)$$

$$\dot{\lambda}_i^v = -\lambda_i^p. \quad (66)$$

Let us assume that at a time $\tau_c > t_i^0$, the vehicle leaves the constrained arc. We denote τ_c^- and τ_c^+ as the immediate left and the right side of τ_c . At this entry point, using the jump conditions (56) and (57), we assess the discontinuities of the costates and the Hamiltonian,

$$\lambda_i^p(\tau_c^-) - \lambda_i^p(\tau_c^+) = \eta_1 \frac{\partial(u_i(\tau_c) - u_{max})}{\partial p_i(t)} = 0, \quad (67)$$

$$\lambda_i^v(\tau_c^-) - \lambda_i^v(\tau_c^+) = \eta_2 \frac{\partial(u_i(\tau_c) - u_{max})}{\partial v_i(t)} = 0, \quad (68)$$

$$H(\tau_c^+) - H(\tau_c^-) = \eta_3 \frac{\partial(u_i(\tau_c) - u_{max})}{\partial t} = 0. \quad (69)$$

From (68), we get

$$u_i(\tau_c^+) = u_i(\tau_c^-) = u_{max}. \quad (70)$$

Using (64),(65), (66), (70), the initial, final conditions, and the terminal transversality condition at $t = t_i^m$, we can formulate a closed form analytic solution similar to (63) by stitching the constrained and unconstrained arcs together at $t = \tau_c$.

Case 3: If both the control constraint $u_i(t) - u_{max} \leq 0$ and state constraint $v_i(t) - v_{max} \leq 0$ are violated, we can derive the analytic solution following the procedure described in the previous two cases. Due to lack of space, only the numerical result is shown in the following section (see Fig. 3).

V. SIMULATION RESULTS

We validate the analytic solution of the constrained optimization problem through numerical analysis in MATLAB. We select the initial and final position as $p_i(t_i^0) = 0$ m and $p_i(t_i^m) = 200$ m, and the initial velocity as $v_i(t_i^0) = 13.4$ m/s. We enforce maximum velocity $v_{max} = 21$ m/s and maximum acceleration $a_{max} = 1.4$ m/s². We present only the cases with the state constraint $v_i(t) - v_{max} \leq 0$ and control constraint $u_i(t) - u_{max} \leq 0$ violation.

Fig. 1 shows the unconstrained optimal trajectory for two different merging time t_i^m of 10 s and 20 s. As described in Lemma 2, we observe two different types of optimal trajectories. This implies that based on the terminal conditions, a CAV may speed up or slow down optimally to satisfy the boundary conditions. We also observed that both the predefined state and control constraints (for $a_i < 0$) are violated in Fig. 1 (top-left and right). We illustrate

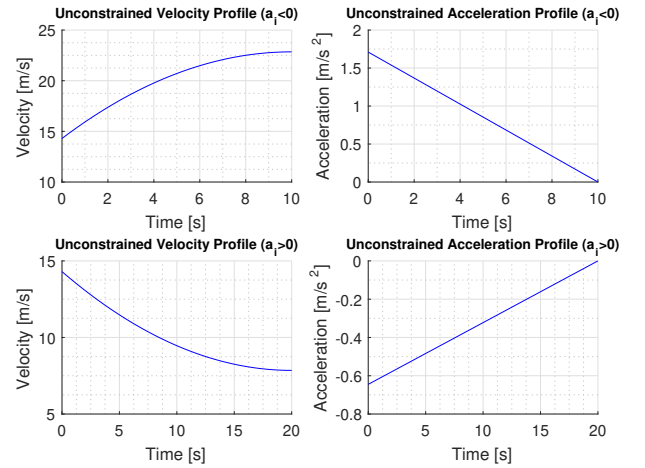


Fig. 1. State and control unconstrained optimal profile for 1) $a_i < 0$ (top) and 2) $a_i > 0$ (bottom) cases.

the optimal state and control trajectories for only state constrained in Fig. 2 (top) and only control constrained in Fig. 2 (bottom) cases. We observe that, when only the state constraint is enforced (see Fig. 2, top-left), the state trajectory transitions from the unconstrained to constrained arc with $v_i(t) = v_{max}$. Note that, in the state constrained solution, the control constraint is violated (Fig. 2, top-right) which was non-existent before, as discussed in theorem 4. Similarly, we observe in Fig. 2 (bottom-right) that the control constrained optimal trajectory creates a possibility of additional state constraint violation (Fig. 2, bottom-left) due to the increased speed, as discussed in Theorem 5. Hence, we need to take the additional constraint violation into account by Theorem 4 and 5, and enforce both state and control constraints if needed. Fig. 3 shows the unconstrained and fully constrained state and control constrained trajectories. The three-point boundary value problem is solved in this case, and two constrained and one unconstrained arcs are pieced together to provide the optimal solution.

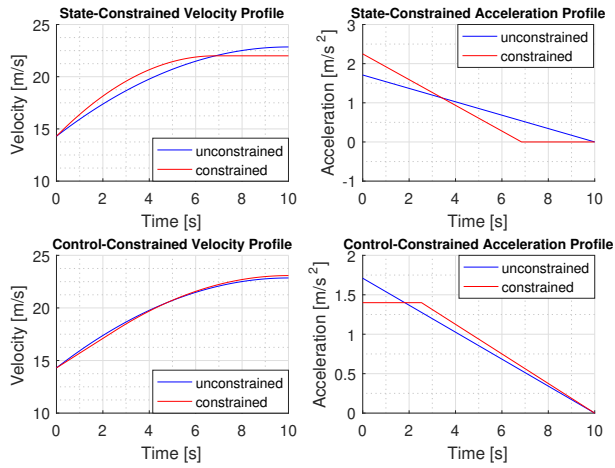


Fig. 2. State constrained optimal velocity (top-left) and acceleration (top-right) profile, and control constrained optimal velocity (bottom-left) and acceleration (bottom-right) profile.

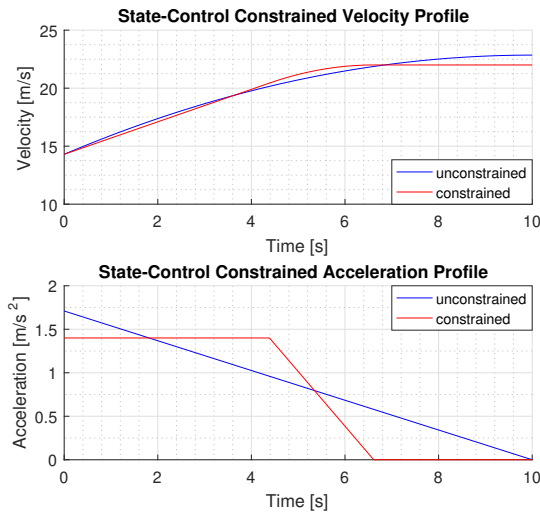


Fig. 3. State and control constrained optimal velocity (left) and acceleration (right) profile.

VI. CONCLUDING REMARKS

In this paper, we addressed the state and control constrained optimal framework for coordinated CAVs. We mathematically quantified the activation of the state-control constraints and provided conditions under which they become active. We derived the closed form analytical solution for the constrained optimization problem and validated a subset of different cases through numerical simulation. Ongoing work includes other cases along with the conditions for the existence of solution along with the terminal speed constrained formulation. The impact of the constrained solution in traffic simulation is also a task for future work.

REFERENCES

[1] R. Margiotta and D. Snyder, "An agency guide on how to establish localized congestion mitigation programs," U.S. Department of Transportation. Federal Highway Administration, Tech. Rep., 2011.

[2] J. Lee, B. B. Park, K. Malakorn, and J. J. So, "Sustainability assessments of cooperative vehicle intersection control at an urban corridor," *Transportation Research Part C: Emerging Technologies*, vol. 32, pp. 193–206, 2013.

[3] A. A. Malikopoulos, C. G. Cassandras, and Y. J. Zhang, "A decentralized energy-optimal control framework for connected automated vehicles at signal-free intersections," *Automatica*, vol. 93, pp. 244 – 256, 2018.

[4] A. A. Malikopoulos and J. P. Aguilar, "An Optimization Framework for Driver Feedback Systems," *IEEE Transactions on Intelligent Transportation Systems*, vol. 14, no. 2, pp. 955–964, 2013.

[5] M. Athans, "A unified approach to the vehicle-merging problem," *Transportation Research*, vol. 3, no. 1, pp. 123–133, 1969.

[6] K. Dresner and P. Stone, "Multiagent traffic management: a reservation-based intersection control mechanism," in *Proceedings of the Third International Joint Conference on Autonomous Agents and Multiagents Systems*, 2004, pp. 530–537.

[7] —, "A multiagent approach to autonomous intersection management," *Journal of artificial intelligence research*, vol. 31, pp. 591–656, 2008.

[8] A. de La Fortelle, "Analysis of reservation algorithms for cooperative planning at intersections," *13th International IEEE Conference on Intelligent Transportation Systems*, pp. 445–449, Sep. 2010.

[9] S. Huang, A. Sadek, and Y. Zhao, "Assessing the Mobility and Environmental Benefits of Reservation-Based Intelligent Intersections Using an Integrated Simulator," *IEEE Transactions on Intelligent Transportation Systems*, vol. 13, no. 3, pp. 1201–1214, 2012.

[10] I. H. Zohdy, R. K. Kamalanathsharma, and H. Rakha, "Intersection management for autonomous vehicles using iCACC," *2012 15th International IEEE Conference on Intelligent Transportation Systems*, pp. 1109–1114, 2012.

[11] F. Yan, M. Dridi, and A. El Moudni, "Autonomous vehicle sequencing algorithm at isolated intersections," *2009 12th International IEEE Conference on Intelligent Transportation Systems*, pp. 1–6, 2009.

[12] K.-D. Kim and P. Kumar, "An MPC-Based Approach to Provable System-Wide Safety and Liveness of Autonomous Ground Traffic," *IEEE Transactions on Automatic Control*, vol. 59, no. 12, pp. 3341–3356, 2014.

[13] J. Rios-Torres and A. A. Malikopoulos, "A Survey on Coordination of Connected and Automated Vehicles at Intersections and Merging at Highway On-Ramps," *IEEE Transactions on Intelligent Transportation Systems*, vol. 18, no. 5, pp. 1066–1077, 2017.

[14] J. Rios-Torres, A. A. Malikopoulos, and P. Pisu, "Online Optimal Control of Connected Vehicles for Efficient Traffic Flow at Merging Roads," in *2015 IEEE 18th International Conference on Intelligent Transportation Systems*, 2015, pp. 2432–2437.

[15] A. M. I. Mahbub, L. Zhao, D. Assanis, and A. A. Malikopoulos, "Energy-optimal coordination of connected and automated vehicles at multiple intersections," in *Proceedings of the American Control Conference*, 2019 (accepted), arXiv:1903.03169.

[16] I. A. Ntousakis, I. K. Nikolos, and M. Papageorgiou, "Optimal vehicle trajectory planning in the context of cooperative merging on highways," *Transportation Research Part C: Emerging Technologies*, vol. 71, pp. 464–488, 2016.

[17] Y. Zhang, A. A. Malikopoulos, and C. G. Cassandras, "Optimal control and coordination of connected and automated vehicles at urban traffic intersections," in *Proceedings of the American Control Conference*, 2016, pp. 6227–6232.

[18] L. Zhao, A. A. Malikopoulos, and J. Rios-Torres, "Optimal control of connected and automated vehicles at roundabouts: An investigation in a mixed-traffic environment," in *15th IFAC Symposium on Control in Transportation Systems*, 2018, pp. 73–78.

[19] A. Stager, L. Bhan, A. A. Malikopoulos, and L. Zhao, "A scaled smart city for experimental validation of connected and automated vehicles," in *15th IFAC Symposium on Control in Transportation Systems*, 2018, pp. 130–135.

[20] A. A. Malikopoulos, S. Hong, B. Park, J. Lee, and S. Ryu, "Optimal control for speed harmonization of automated vehicles," *IEEE Transactions on Intelligent Transportation Systems*, 2018 (in press).

[21] I. M. Ross, *A Primer on Pontryagin's Principle in Optimal Control*. Collegiate Publishers, 2015.

[22] A. E. Bryson and Y. C. Ho, *Applied optimal control: optimization, estimation and control*. CRC Press, 1975.